Research Article **ISSN: 2395 – 5597**

International Journal of Engineering and Robot Technology

Journal home page: www.ijerobot.com

PERFORMANCE ANALYSIS OF PULMONARY LOBE SEGMENTATION USING WATER SHED TRANSFORMATION AND FCM

S. Swarnasaji*[1]

*[1]Department of Computer Science Engineering, Arul College of Technology, Radhapuram, Tamilnadu, India.

ABSTRACT

In this work, an automated segmentation approach is presented that performs a FCM (Fuzzy C Means) on computed tomography (CT) scans to subdivide the lungs into lobes. FCM is used to segment boundary of region accurately. A marker based watershed transformation is also computed on tomography (CT) scans to subdivide the lungs into lobes. The cost image for the watershed transformation and FCM is computed by combining information from fissures, bronchi and pulmonary vessels. Finally identify the best performance of the image between FCM and watershed transformation. Lung lobe segmentation is relevant in clinical applications particularly for treatment planning. The location and distribution of pulmonary diseases are important parameters for the selection of a suitable treatment. Locally distributed emphysema can be treated more effective by lobar volume resection than homogeneously distributed emphysema. Another application is quantitative monitoring of pulmonary diseases such as emphysema or fibrosis. A lobe-wise analysis shows the progression of the disease in more detail.

KEY WORDS

Fissure segmentation, Lunglobe segmentation, Watershed segmentation and Fuzzy C-Means.

Author of correspondence:

S. Swarnasaji,
Department of Computer Science Engineering,
Arul College of Technology,
Radhapuram, Tamilnadu, India.

Email: sajiswarnasaras@gmail.com

INTRODUCTION[1]

The human lungs are subdivided into five lobes that are separated by visceral pleura called pulmonary fissure. There are three lobes in the right lung, namely upper, middle, and lower lobe. The right upper and right middle lobe are divided by the right minor fissure whereas the right major fissure delimits the lower lobe from the rest of the lung. In the left lung there are only two lobes, the upper and the lower lobe, that are divided by the left major fissure. A characteristic of the pulmonary lobes are

separated supply branches for both vessels and airways[1-3].

Lung lobe segmentation is relevant in clinical applications particularly for treatment planning. The location and distribution of pulmonary diseases are important parameters for the selection of a suitable treatment. Locally distributed emphysema can be treated more effective by lobar volume resection than homogeneously distributed emphysema. Another application is quantitative monitoring of pulmonary diseases such as emphysema or fibrosis. A lobe-wise analysis shows the progression of the disease in more detail[4]. Computed tomography (CT) allows visualization of the lungs within a few seconds. Since typical scans with high anatomical details contain over 400 slices with sub millimeter resolution for each direction, manual segmentation is time consuming and there is demand for automatic lung lobe segmentation methods[5].

Related Works[6-10]

Based on computed tomography (CT) scans[3], the following steps are performed. 1) The volume data is preprocessed and the vessels are segmented. 2) The skeleton of the vessels is determined and transformed into a graph enabling a geometrical and structural shape analysis. Using this information the different intrahepatic vessel systems are identified automatically. 3) Based on the structural analysis of the branches of the portal vein, their vascular territories are approximated with different methods. These methods are compared and validated anatomically by means of corrosion casts of human livers. 4) Vessels are visualized with graphics primitives fitted to the skeleton to provide smooth visualizations without aliasing artifacts.

Fissure detection is accomplished in two stages: an initial fissure search and a final fissure search. A fuzzy reasoning system is used in the fissure search to analyze information from three sources: the image intensity, an anatomic smoothness constraint, and the atlas-based search initialization[11].

Segmentation of Pulmonary Lobes

The segmentation of pulmonary lobes is challenging because of anatomical variation and incomplete fissures[8]. On the one hand, pathologies can deform the lobes and make the fissures unrecognizable. And on the other hand, even in patients with normal lung parenchyma the fissures are often not complete; these are examples of incomplete and deformed fissures. For cases with incomplete fissures radiologists infer the lobar boundaries using information from the bronchi and vessel trees. Since there are usually no major supply branches between the lung lobes the lobar boundaries are defined in between the bronchi and vessel branches[4].

Automatic lung and Lung Lobe Segmentation

It is a framework for automatic lung and lung lobe segmentation. The lobe segmentation was based on a watershed transformation that takes an analysis of lobar airways and vasculature into account. It was robust against missing fissures but therefore frequently inaccurate at clearly visible fissures. The method had been applied to more than 1000 dataset but was not quantitatively validated[1].

Pulmonary Lobe Segmentation

Here it presented pulmonary lobe segmentation similar to Kuhnig K *et al*. In the first step, the lobes were segmented by a watershed transformation based on a distance map of the vasculature and markers from the labeled bronchi tree. In the second step, a 3-D optimal surface detection was performed in a region of interest (ROI) around the initial segmented fissures to refine the lobe boundaries. As a last step, incomplete fissures were extrapolated based on a fast-marching method[7].

PROPOSED SYSTEM[12-19]

Prerequisite Segmentations

In the first step lungs are segmented since all other segmentations are only performed inside the lung regions. A good lung segmentation is a prerequisite for the here presented lobe segmentation approach. The lung segmentation applied achieved the best performance in the LOLA11 challenge. It is based on previous work and therefore not described in this paper. Describe the segmentation of the vessels, fissures, and bronchi. Note that any vessel, airway, or fissure segmentation could be plugged into the method without adaptation[1] (Figure No.1).

Pulmonary Vessels

Based on the assumption that there are usually no major vessels at the lobar boundaries[1], the distance

to the pulmonary vasculature is a suitable feature to detect lobar boundaries. Before thresholding a downscaling with clamping is applied to reduce memory requirements. With the following equation the dataset V_{orig} is scaled down to the 8-bit range [0, 255] where 255 marks voxels outside the lung mask L.

$$v_{ds} = \begin{cases} \max\left(0, \min\left(254, \frac{V_{orig} + 1024}{4}\right)\right), & x < 0 \\ 255, & \text{otherwise} \end{cases}$$

The resulting dataset V_{ds} is threshold to receive the vessel mask V

$$V = 130 \leq v_{ds} \leq 255$$

After the thresholding, a connected component analysis filters out structures with a volume of less than 2 ml to separate the interconnected vasculature from smaller, isolated high-density structures such as thickened parts of the fissures.

Pulmonary Fissures

The first step of the fissure segmentation process is an enhancement of the fissures based on the eigen values of the Hessian matrix that gives a fissure probability for each voxel. Fissures can locally be modeled as a sheet where the eigen value orthogonal to the fissure plane is large, and the other two eigen values are small[1].

$$F_{Structure} = \ominus(-\lambda_3)e^{-(\lambda_3-\alpha)^6/\beta^6}$$
$$F_{Sheet} = e^{-\lambda_2^6/\gamma^6}$$

Bronchi

In CT images[3], the airway lumen is dark and separated from the parenchymal tissue by thin airway wall structures that appear brighter. First, to reduce noise, a Gaussian smoothing with fixed kernel width is applied to the image although the blurring increases the partial volume related problems. Second, a bronchi enhancement filtering is applied to the blurred image. Partial volume effects and the additional Gaussian blurring let the lumen of small airways appear brighter than normal air. The goal of the bronchi enhancement filtering is to detect voxels that are surrounded by dense circular structures as bronchi and to revert these volume averaging effects by decreasing their density again.

System Architecture

Architecture diagram shows 3-D (Figure No.2) region growing algorithm is used to extract the airway lumen from the preprocessed image. The region growing is initialized by detecting the trachea. A 2-D connected component analysis of the airspace mask finds trachea candidates and the components that overlap in z-direction are selected to be the trachea. Starting from the position of the minimum gray value within the trachea, the segmentation threshold is iteratively increased and the segmentation volume is monitored. It from the original chest CT scan four features is extracted to calculate the cost image for the watershed transformation. Then distance calculator between blood vessel masked out, pulmonary vasculature, bronchial tree and pulmonary fissure. All the four inputs are equally weighted to uptime to cost image for FCM[19]. Finally compute how FCM has better performance than watershed Transformation.

Lung lobe segmentation is relevant in clinical applications particularly for treatment planning. The location and distribution of pulmonary diseases are important parameters for the selection of a suitable treatment. Locally distributed emphysema can be treated more effective by lobar volume resection than homogeneously distributed emphysema. Another application is quantitative monitoring of pulmonary diseases such as emphysema or fibrosis. A lobe-wise analysis shows the progression of the disease in more detail.

Watershed-Based Lobe Segmentation

The anatomical information of fissures, bronchi, and vessels are combined into a cost image for watershed-based lobe segmentation[1]. To obtain these inputs for a chest CT scan in which the vessels, fissures, and bronchi have been segmented the following steps are performed: 1) the segmentations are combined into a cost image, 2) markers for the

watershed are computed, and 3) the lobes are segmented using a 3-D watershed transformation and post processing is applied.

Markers for the Watershed Segmentation

Markers should ideally be created equally distributed throughout the lobes to get a good coverage of the lobe areas[1]. To generate the markers, the different sub trees belonging to the lobes and lobar segments are identified in the airway tree. This is done by searching for major bifurcations separating large sub trees in appropriate orientations. In the first step a directed graph is modeled from the bronchi tree with the trachea as root. The center of gravity and volume of the segmented voxels[14] are calculated for each sub tree.

Fuzzy C-Means (FCM)

The algorithm is developed by modifying the objective function of the standard FCM algorithm with a penalty term that takes into account the influence of the neighboring pixels on the centre pixels. The penalty term acts as a regularizer in this algorithm, which is inspired from the neighborhood expectation maximization algorithm and is modified in order to satisfy the criterion of the FCM algorithm[18,19]. The performance of our algorithm is discussed and compared to those of many derivatives of FCM algorithm. Experimental results on segmentation of synthetic and real images

$$y_j = \frac{\sum_{i=1}^{n} u_{ij}^{m} x_i}{\sum_{i=1}^{n} u_{ij}^{m}} \quad \text{.....(3)}$$

The FCM algorithm is iterative and can be stated as follow:

1. Select m(m > 1); initialize the membership function values μ_{ij}, i = 1,2,...,n; j = 1,2,...,c.
2. Compute the cluster centers y_j , j = 1,2,..., ,c .
3. Compute Euclidian distance d_{ij}, i=1,2…,n j=1,2,…,c.

Cost Image Construction

The first feature is derived from the segmentation of the vascular tree. The normalized result is a feature image V_{cost} in the range of [0, 255] that shows high values in the region of the lobar boundaries. Since the fissures are the physical boundaries between the lobes, on locations where they are present they demonstrate that the proposed algorithm is effective and robust.

FCM partitions a set of n objects x {x , x ,..., xn} in R^d dimensional space into c(1 < c < n) fuzzy clusters with y = {y_1, y_2 , y_3 ,..., y_c} cluster centers or centroids. The fuzzy clustering of objects is described by a fuzzy matrix μ with n rows and c columns in which n is the number of data objects and c in the number of clusters. M_{ij} , the element in the i^{th} row and j^{th} column in μ , indicates the degree of association or membership function of the ith object with the jth cluster[11].

The objective function of FCM algorithm is to minimize the following equation.

$$J_m = \sum_{j=1}^{c} \sum_{i=1}^{n} u_{ij}^{m} d_{ij} \quad \text{.....(1)}$$

Where

$$d_{ij} = \|x_i - y_j\| \quad \text{.....(2)}$$

In this survey there are various latest techniques used in image segmentation which are very useful in medical field for diagnosis of a problem. m(m > 1) is a scalar termed as weighting exponent. M controls the fuzziness of the resulting clusters and dij is the Euclidian distance from object i x to the cluster center y j. The y_j, centroid of the j^{th} cluster, is obtained as:

indicate the exact lobar boundary and should be emphasized[1]. Thus, to get the feature image F_{cost} in the range of [0, 255] with high values at the fissures, is squared, inverted, and normalized

$$F_{cost} = 255.(1 - (v/v_{max})^2 \quad \text{.....(4)}$$

Where v_{max} is the maximum value of the image.

The last feature is based on the observation that due to the small of the fissure enhancement filter pathological thick fissures are not always detected by the fissure segmentation. In high-resolution chest CT scans the fissures, and especially pathological thick fissures, show higher density than the surrounding lung parenchyma. Thus the fourth feature O_{cost} is the original CT scan V_{orig}, normalized and clamped to the range [0, 255]. The vasculature is masked out since vessels usually show even higher density than thick fissures.

$$O_{cost} = \begin{cases} \max\left(0, \min\left(255, \frac{V_{orig} + 1024}{4}\right)\right), & \neq V \\ 0, & otherwise \end{cases} \quad \text{.....(5)}$$

In order to obtain the final cost image, the four features are combined with equal weight

$$Cost = \frac{V_{cost} + B_{cost} + F_{cost} + O_{cost}}{4} \quad \text{.....(6)}$$

By combining the four input features false positive responses of individual features are reduced since those areas that have a high value in all individual cost images are enhanced.

Lobe Segmentation and Post processing

To obtain lobe segmentation from the cost image cost and the markers, the 3-D watershed transformation proposed by [1] is performed. Down sampling of the cost image to a resolution of 1.5mm X 1.5mm X 1.5mm is applied to reduce calculation time. The applied water shed algorithm separates regions with local maxima in between and can be used with an arbitrary number of markers. The borders between the obtained lobes after the watershed segmentation are not always smooth due to local variations in the cost image.

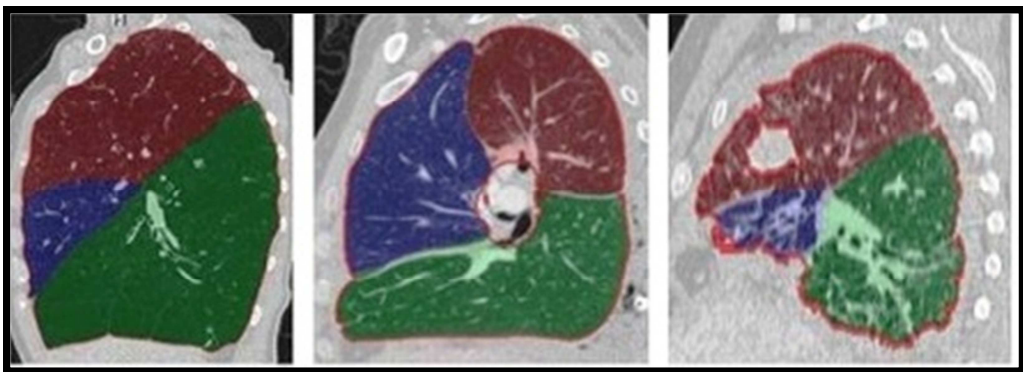

Figure No.1: Anatomical variation of pulmonary lobes slices with labeled lobes Red = upper lobe, Blue = middle lobe, Green = lower lobe

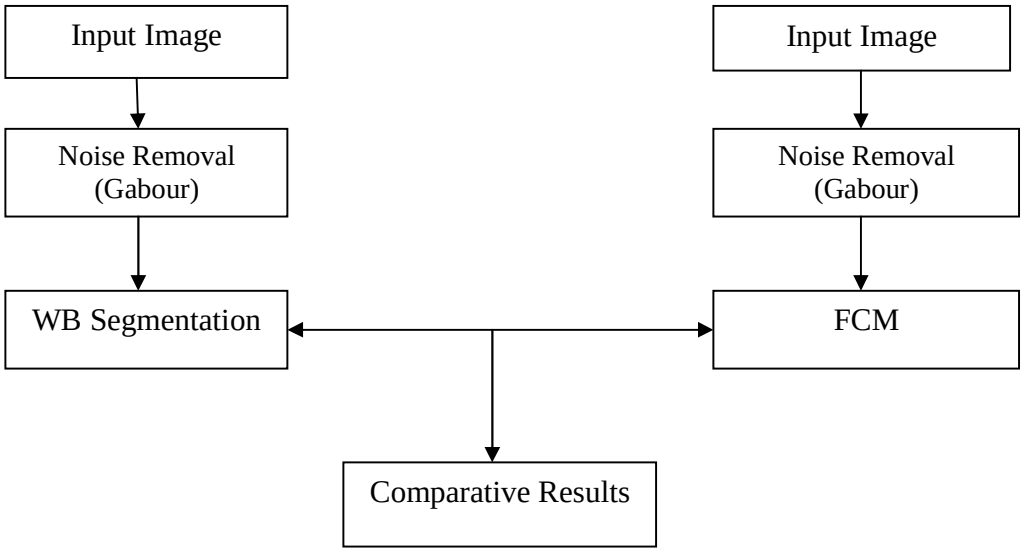

Figure No.2: System Architecture

CONCLUSION

In conclusion, I have presented a fast automatic lobar segmentation method and shown in an extensive series of experiments with 75 CT scans that the method performs well and is robust against missing fissures. Pathological thick fissures are sometimes not detected as fissures but as vessels. Thus, for these cases the lobe segmentation does not exactly follow the lobar fissures. The weight of the fissures in the cost image is equal to the weights of the other inputs. Such a low weight allows a high degree of independence against missing fissures compared to a higher weight which can increase the accuracy of the segmentation. For future work we want to set the weight of the inputs of the cost image dynamically based on a confidence estimation of the vessel, bronchi, and fissure segmentation. Future work will focus on adaptively deciding the penalized parameter of this algorithm as well as compensating for the intensity in homogeneity while segmenting the image data.

ACKNOWLEDGEMENT

The authors are highly thankful to Arul College of technology, Radhapuram, India for providing all the facilities to carry out this work.

CONFLICT OF INTEREST

We declare that we have no conflict of interest.

BIBLIOGRAPHY

1. Bianca Lassen, Eva M. van Rikxoort, Michael Schmidt, Sjoerd Kerkstra, Bram van Ginneken and Jan-Martin Kuhnigk. “Automatic Segmentation of the Pulmonary Lobes from Chest CT Scans Based on Fissures, Vessels, and Bronchi,” *IEEE Transactions On Medical Imaging*, 32(2), 2013, 210-222.
2. Lassen B, Kuhnigk J M, Schmidt M, Krass S and Peitgen H O. “Lung and lung lobe segmentation methods at fraunhofer mevis,” *presented at the 4th Int. MICCAI Workshop Pulmonary Image Anal., Toronto, Canada*, Sep. 2011.
3. Eva M. van Rikxoort, De Hoop B, Van de Vorst S, Prokop M and Bram van Ginneken. “Automatic segmentation of pulmonary segments from volumetric chest CT scans,” *IEEE Trans. Med. Imag*, 28(4), 2009, 62-630.
4. Eva van Rikxoort, Prokop M, De Hoop B, Viergever M, Pluim J and Van Ginneken B. “Automatic segmentation of pulmonary lobes robust against incomplete fissures,” *IEEE Trans. Med. Imag.*, 29(6), 1286-1296.
5. Eva. van Rikxoort, Van Ginneken B, Klik M and Prokop M. “Supervised enhancement filters: Application to fissure detection in chest CT scans,” *IEEE Trans. Med. Imag.*, 27(1), 2008, 1-10.
6. Wang J, Betke M and Ko J P. “Pulmonary fissure segmentation on CT,” *Med. Image Anal.*, 10(4), 2006, 530-547.
7. Kuhnigk J M, Dicken V, Zidowitz S, Bornemann L, Kuemmerlen B, Krass S, Peitgen H O, Yuval S, Jend H H, Rau W S and Achenbach T. “New tools for computer assistance in thoracic CT-Part I: Functional analysis of lungs, lung lobes, and bronchopulmonary segments,” *Radio Graphics*, 25(2), 2005, 525-536.
8. Pu J, Leader J, Zheng B, Knollmann F, Fuhrman C, Sciurba F and Gur D. “A computational geometry approach to automated pulmonary fissure segmentation in CT examinations,” *IEEE Trans. Med. Imag.*, 28(5), 2009, 710-719.
9. Jia-Yin Kang, Cheng-Long Gong, Wen-Juan Zhang. “Fingerprint image segmentation using modified fuzzy c-means algorithm”, *J. Biomedical Science and Engineering*, 2, 2009, 656-660.
10. Gülsün M, Ariyürek O, Cömert R and Karabulut N. “Variability of the pulmonary oblique fissures presented by high-resolution computed tomography,” *Surg. Radiol. Anat.*, 28, 2006, 293-299.
11. Mahesh Yambal, Hitesh Gupta. “Image Segmentation using Fuzzy C Means Clustering: A survey”, *International Journal of Advanced Research in Computer and*

Communication Engineering, 2(7), 2013, 2927-2929.

12. Noordam J C, Van den Broek, Buydens W H A M. "L.M.C.: Geometrically Guided Fuzzy C-Means Clustering for Multivariate Image Segmentation", *Proc. International Conference on Pattern Recognition*, 1, 2000, 462-465.
13. Sverzellati N, Calabro E, Randi G, La Vecchia C, Marchiano A, Kuhnigk J M, Zompatori M, Spagnolo P and Pastorino U. "Sex differences in emphysema phenotype in smokers without airflow obstruction, *Eur. Respirat. J.*, 33(6), 2009, 1320-1328.
14. Wei Q, Hu Y, Mac Gregor J and Gelfand G. "Automatic recognition of major fissures in human lungs," *Int. J. Comput. Assist. Radiol. Surg.*, 7(1), 2012, 111-123.
15. Wiemker R, Buelow T and Blaffert T. "Unsupervised extraction of the pulmonary interlobar fissures from high resolution thoracic CT data," *Comput. Assist. Radiol. Surg.*, 1281, 2005, 1121-1126.
16. Ukil S and Reinhardt J M. "Anatomy-guided lung lobe segmentation in x-ray CT images," *IEEE Trans. Med. Imag.*, 28(2), 2009, 202-214.
17. Songcan Chen and Daoqiang Zhang. "Robust Image Segmentation Using FCM With Spatial Constraints Based On New Kernel-Induced Distance Measure", *IEEE Transactions On Systems, Man, and Cybernetics-Part B: Cybernetics*, 34(4), August 2004.
18. Soumajit Pramanik, Amiya Halder, Arindam Kar, "Dynamic Image Segmentation using Fuzzy C-Means based Genetic Algorithm", *International Journal of Computer Applications*, 28(6), 2011, 15-20.
19. Yong Yang and Shuying Huang. "Image Segmentation by Fuzzy C-Means Clustering Algorithm with A Novel Penalty Term", *Computing and Informatics*, 26, 2007, 17-31.

Please cite this article in press as: S. Swarnasaji. Performance Analysis of Pulmonary Lobe Segmentation using Water Shed Transformation and FCM, *International Journal of Engineering and Robot Technology*, 1(1), 2014, 18 - 24.